Pramāṇa, Vol. 15, No. 5, November 1980, . 449-461. © Printed in India.

Microscopic band-mixing calculations in ^{154,156}Gd

S V MOHOLKAR, C S WARKE and M R GUNYE*
Tata Institute of Fundamental Research, Homi Bhabha Road, Bombay 400 005, India
*Bhabha Atomic Research Centre, Trombay, Bombay 400 085, India

MS received 9 June 1980; revised 23 September 1980

Abstract. A many-body microscopic band-mixing formulation of variation after projection of angular momentum and conservation of nucleon number is used to study the yrast band and first excited $K^\pi = 0^+$ band in the doubly even nuclei ^{154,156}Gd. The computed energy spectra and the interband and intra-band B (E2) values are in good agreement with corresponding experimental data. Connection with the phenomenological model of Stephens and Simon is discussed, bringing out the role played by the $i_{13/2}$ neutron pair in the microscopic formalism.

Keywords. Nuclear structure; ^{154,156}Gd; yrast band; first excited band; energy spectra; interband and intraband B(E2) values; band-mixing; angular momentum projection; conservation of nucleon number.

1. Introduction

The backbending phenomenon exhibited by many rare-earth nuclei has been a topic of interest for nuclear physicists in recent years. The phenomenological rotation alignment (RAL) model of Stephens and Simon (1972) explains the backbending in terms of band-crossing, where a band built on a decoupled $oi_{13/2}$ neutron pair crosses the ground band and backbending of the yrast band takes place. The anomalous backbending phenomenon is attributed by Mottelson and Valatin (1960) to the vanishing of the pairing correlations due to Coriolis force. There are theoretical approaches (Kumar 1972; Banerjee *et al* 1973; Nair and Ansari 1973; Krumlinde and Szymanski 1974) based essentially on the approximate angular momentum projection which qualitatively explain the phenomenon. The microscopic analysis of the processes responsible for backbending is of added importance because of the observations that not only the yrast band but also the yrare band in some nuclei exhibits backbending. The variational method with angular momentum projection has been successfully used to study the yrast states of a few rare-earth nuclei (Faessler *et al* 1974; Warke and Gunye 1975, 1976). In addition to angular momentum projection there is yet another complication due to number projection (Grummer *et al* 1975; Gunye and Warke 1979) from the pair-correlated state. It is found (Gunye and Warke 1979) that the number conservation in each angular momentum state is essential for a good agreement between theoretical and experimental results.

In this paper, we report the results of our study of ^{154,156}Gd using the variation after projection (VAP) method. The nuclei are chosen with a view to understand the role played by $i_{13/2}$ neutron-pair in the rare-earth region. We have, in addition, incorporated a band-mixing formulation to obtain the energy spectra of the two

lowest $K^\pi = 0^+$ bands and also the interband and intraband $B(E2)$ values. Such a band-mixing microscopic calculation to investigate the structure of the yrast and yrare bands of rare-earth nuclei is not reported in literature so far. In the present investigations, we have also attempted to find the connection between the phenomenological RAL model (Stephens and Simon 1972) and the microscopic VAP formalism.

The theoretical formulation is outlined in § 2, the results are presented and discussed in § 3 and the conclusions are given in § 4.

2. Theoretical formulation

2.1 *Expressions for energy and B(E2)*

It is obvious that for realistic nuclear structure calculations of heavy nuclei in the rare-earth region from microscopic many-body theory, one would have to use a large configuration space. The computational difficulties involved in performing the projected Hartree-Fock-Bogoliubov (HFB) calculations in large configuration space can be somewhat reduced by using a simpler many-body Hamiltonian. In this paper, we employ the quadrupole plus pairing interaction Hamiltonian, whose parameters are determined by Kumar and Baranger (1968) from their study of equilibrium deformations of heavy nuclei.

$$H = \sum_{\alpha} \epsilon_\alpha \, a_\alpha^\dagger \, a_\alpha - \tfrac{1}{2} \, \chi \sum q_{\alpha\gamma}^{\mu} \, q_{\delta\beta}^{\mu} \, a_\alpha^\dagger \, a_\beta^\dagger \, a_\delta \, a_\gamma$$

$$- \tfrac{1}{2} \, G \sum (-1)^{j_\alpha - m_\alpha + j_\gamma - m_\gamma} \, a_\alpha^\dagger \, a_{\bar{\alpha}}^\dagger \, a_{\bar{\gamma}} \, a_\gamma, \qquad (1)$$

where q^μ is the quadrupole operator and χ and G are the strengths of the quadrupole and pairing interactions respectively. The subscript α in equation (1) denotes all the quantum numbers $(n_\alpha, l_\alpha, j_\alpha, m_\alpha)$ necessary for the specification of a spherical single-particle state with energy ϵ_α. The state $\bar{\alpha}$ is connected to the state α by time-reversal operator. The sums in eq. (1) run over the entire configuration space.

We consider the intrinsic variational wave function to be axially symmetric in view of the fact that the nuclei under investigation are found (Das Gupta and Preston 1963; Gunye *et al* 1964; Kumar and Baranger 1968) to prefer axially symmetric equilibrium deformation. The trial variational wave function is taken to be the good angular momentum state projected from the intrinsic B.C.S. state Φ_0 (β, Δ_p, Δ_n, λ_p, λ_n) of the A-nucleon system. The deformation β, the pairing gaps Δ_p (for protons) and Δ_n (for neutrons) and the chemical potentials λ_p (for protons) and λ_n (for neutrons) are the variational parameters for each angular momentum state J. The chemical potentials in any state J are determined such that the number of nucleons in the projected state is equal to the actual number of nucleons in the nucleus. The wave function Ψ_M^J (β, Δ_p, Δ_n, λ_p, λ_n) projected from the intrinsic state Φ_0 is given by

$$\Psi_M^J = P_{\mathrm{MO}}^J \, \Phi_0, \qquad (2)$$

where P^J_{MO} is the angular momentum projection operator.

The expectation value E^J of the Hamiltonian of equation (1) in the projected state J of equation (2) can be expressed (Warke and Gunye 1976) as

$$E^J(\beta, \Delta_p, \Delta_n, \lambda_p, \lambda_n) = h^J/p^J, \tag{3}$$

where
$$h^J \equiv (J+\tfrac{1}{2}) \int_0^\pi d^J_{00}(\theta)\,[\det W]^{1/2}\, X(\theta) \sin\theta\, d\theta, \tag{4}$$

$$X(\theta) = 2\sum \epsilon_t\, \rho_{t+t+} - G\left(\sum \sigma_{t+t-}\right)^2 - \tfrac{1}{2}\chi\,(Q^2_{0+} + 2\,Q^2_{2+} + 2\,Q^2_{1-}), \tag{5}$$

and p^J is obtained from (4) by replacing $X(\theta)$ by unity. The overlap matrix W in (4) and the generalised density matrices ρ and σ in (5) depend (Warke and Gunye 1976) on the transformation coefficients of deformed single particle orbits in terms of the spherical basis states, the rotation matrix $d(\theta)$ and the occupation probabilities of the single particle orbits in the intrinsic state Φ_0. The quantities $Q_{\mu\pm}$ in (5) are given by

$$Q_{\mu\pm} = \sum \left(q^\mu_{t\pm\, j+} + q^\mu_{j+\, t\pm}\right) \rho_{j+\, t\pm}. \tag{6}$$

The subscript (+ and −) in equations (5) and (6) indicates the states from two subsets that are connected by the time-reversal operator. The number of protons Z^J and neutrons N^J in the projected state with angular momentum J is obtained by evaluating the integral

$$I^J(\beta, \Delta_p, \Delta_n, \lambda_p, \lambda_n) = (J+\tfrac{1}{2})\,(p^J)^{-1} \int_0^\pi d^J_{00}(\theta)\,[\det W]^{1/2} \times \Sigma\, \rho_{t+t+} \sin\theta\, d\theta. \tag{7}$$

The summation in equation (7) over proton (neutron) states gives the proton (neutron) number $Z^J(N^J)$. Finally, the expression for the $B(E2;\, J_i \to J_f)$ value can also be easily derived and is given by

$$B(E2;\, J_i \to J_f) = \frac{2J_f+1}{2J_i+1}\,(p^{J_i} p^{J_f})^{-1}\,[Q(J_i \to J_f)]^2, \tag{8}$$

where
$$Q(J_i \to J_f) = \sum_{\nu=0}^{2} (2-\delta_{\nu 0})\,(J_i\, \nu,\, 2-\nu \,|\, J_f\, 0) \times (J_i+\tfrac{1}{2}) \int_0^{\pi/2} d^{J_i}_{-\nu,\,0}(\theta)\,(Q_{\nu+} + Q_{\nu-})\,[\det W]^{1/2} \sin\theta d\theta. \tag{9}$$

Here $(J_i\nu,\, 2-\nu \,|\, J_f\, 0)$ is the Clebsch-Gordon coefficient and $Q_{\nu\pm}$ is given by (6).

2.2 *Band-mixing formulation*

In the intrinsic wave functions of the ground band of the two nuclei ^{154,156}Gd under investigation, it is found that the last occupied proton orbital is energetically very close to the next excited proton orbital. These two near-degenerate single-particle deformed orbitals f and f' near the Fermi surface are used to construct the orthogonal intrinsic states $\phi_0(f)$ and $\phi_0(f')$ defined by

$$\phi_0(f) = b_f^\dagger b_{\bar{f}}^\dagger \phi_0(ff'),$$

$$\phi_0(f') = b_{f'}^\dagger b_{\bar{f}'}^\dagger \phi_0(ff'), \tag{10}$$

where $$\phi_0(ff') = \prod_{i \neq ff'} (u_i + v_i b_i^\dagger b_{\bar{i}}^\dagger) \mid 0 \rangle.$$

The intrinsic wave function is then taken to be

$$\Phi_0 = A\phi_0(f) + A' \phi_0(f'), \tag{11}$$

with $A^2 + A'^2 = 1$, so that $\langle \Phi_0 \mid \Phi_0 \rangle = 1$. The energy E^J in the projected state $\psi_M^J = P_{M0}^J \Phi_0$ is given by

$$E^J = \langle \psi_M^J \mid H \mid \psi_M^J \rangle / \langle \psi_M^J \mid \psi_M^J \rangle, \tag{12}$$

and this can be evaluated in terms of the matrix elements

$$p_{ff'}^J = \langle \phi_0(f) \mid P_{00}^J \mid \phi_0(f') \rangle,$$

$$h_{ff'}^J = \langle \phi_0(f) \mid HP_{00}^J \mid \phi_0(f') \rangle. \tag{13}$$

Minimising E^J with respect to the coefficients A and A', one obtains a quadratic equation

$$(p_{ff}^J E^J - h_{ff}^J)(p_{f'f'}^J E^J - h_{f'f'}^J) - (p_{ff'}^J E^J - h_{ff'}^J)^2 = 0, \tag{14}$$

to determine E^J. The lower of the two values of E^J is associated with the yrast band and the higher with the yrare band. The band-mixing coefficient B^J for the state J is given by

$$B^J \equiv \left(\frac{A'^J}{A^J}\right) = -\left(\frac{h_{ff}^J - E^J p_{ff}^J}{h_{ff'}^J - E^J p_{ff'}^J}\right). \tag{15}$$

It is clear that the two states of same J in the yrast and yrare bands have different B^J as their energies are different. The intrinsic states of the levels in the yrast and yrare bands are characterised by their band-mixing ratios. The wave functions Ψ^J_M are then used to evaluate the interband and intra-band $B(E2)$ values.

2.3 *Renormalisation procedure*

The parameters χ and G of the Hamiltonian in equation (1) employed in the present calculations are determined from the consideration of the intrinsic states of the deformed nuclei in the region of interest. The values of these parameters are estimated (Kumar and Baranger 1968) by considering the configuration space of two major shells ($N = 4$, 5) for protons and ($N = 5$, 6) for neutrons and assuming an inert core with 40 protons and 70 neutrons. The assumption of inert core necessitates the modification of the nucleon charges and the excitation energies obtained by using projected states. The simplest way to incorporate the effect of the neglected core on the projected energies is by renormalising the calculated energy spectra. We achieve it by introducing a parameter, namely the moment of inertia I_{core} of the core. We assume that the moment of inertia of the nucleus in state J is the sum of the moment of inertia I_{core} of the core and the moment of inertia I^J_{calc} of the outer nucleons. It is reasonable to assume that the core moment of inertia is independent of J for atleast a set of states. The moment of inertia I^J_{calc} of the outer nucleons, however, depends on J, as deduced from the computed energies, E^J_{calc}. Thus

$$E^J_{\text{calc}} = \frac{\hbar^2}{2I^J_{\text{calc}}} \cdot J(J+1). \tag{16}$$

The corrected or normalised energy is then given by

$$E^J_{\text{norm}} = \frac{\hbar^2 J(J+1)}{2(I_{\text{core}} + I^J_{\text{calc}})}. \tag{17}$$

A few remarks about the choice of the parameter I_{core} are in order. This parameter is introduced to take into account the effect of the neglected core on the energy spectra calculated by using only the valence nucleons. This parameter will depend on the core-nucleons as well as on the valence nucleons and their deformed orbits. The I_{core} value can thus be different for different nuclei. Furthermore, it can be different, for different (yrast and yrare) bands within a nucleus, since the intrinsic structure of the two bands is different. Also, the I_{core} value can be different for low-J and high-J states within a band of a nucleus because the deformed orbits occupied by the valence nucleons near the Fermi surface can be different for the two sets of states. It is found, in general, that any value of I_{core} within a small range of $\pm 1\hbar^2$/MeV can reproduce the experimental energy spectrum reasonably well. We have used suitable I_{core} values to obtain an overall good agreement with the states of two bands in $^{154, 156}$Gd under consideration.

The static quadrupole moments $Q(J)$ and the $B(E2; J+2 \rightarrow J)$ values are computed by ascribing the effective charges $e_p = (1+1{\cdot}5\, Z/A)e$ to the protons and $e_n = (1{\cdot}5\, Z/A)e$ to the neutrons to simulate the configuration truncation and core polarisation effects (Kumar and Baranger 1968). The intrinsic quadrupole moment Q_0 is extracted from the calculated $Q(J)$ and $B(E2; J+2 \rightarrow J)$ values by employing the following relations

$$Q_0(Q) = -\left(\frac{2J+3}{J}\right) Q(J), \tag{18}$$

$$Q_0(E2) = \left[\frac{32\pi}{15} \frac{(2J+3)(2J+5)}{(J+1)(J+2)} B(E2; J+2 \rightarrow J)\right]^{1/2}. \tag{19}$$

3. Results and discussion

We first study the ground band with zero quasi-particles (qp). For each angular momentum J, the parameters β, Δ_p, Δ_n, λ_p and λ_n are determined by minimising the projected energy and conserving the nucleon numbers. The numbers Z^J and N^J computed from equation (7) are very sensitively dependent on λ_p and λ_n. Consequently, it is necessary to incorporate very fine variations in λ_p and λ_n in the variational procedure to obtain the correct number in each state J. In the calculations reported in this paper, we have achieved an accuracy upto the fourth decimal place in the numbers computed in each state. This procedure of energy minimisation and number conservation determines the nature of the intrinsic state for each angular momentum J. It is found that two positive parity proton orbitals just at the Fermi surface are almost equally occupied in the zero qp intrinsic state in both the nuclei $^{154, 156}$Gd under investigation here. These two proton orbitals are nearly degenerate in energy with the difference of $\sim 0{\cdot}05$ MeV in energy. Moreover, the near-degeneracy of these two orbitals near the proton Fermi surface persists for all J values, though β, Δ_p and Δ_n change. These proton orbitals characterised by $\Omega = \pm 5/2$ with largest amplitude ($\sim 96\%$) of $0g_{7/2}$ and $\Omega = \pm 3/2$ with largest amplitude ($\sim 87\%$) of $1d_{5/2}$ are employed in constructing the states $\phi_0(f)$ and $\phi_0(f')$ in the present calculations. This choice of the two-proton orbitals in our calculations does not automatically mean that the observed features in the energy spectra of ^{154,156}Gd are attributed to these proton quasiparticles. These orbitals merely define two bands which are admixed in the band-mixing formulation to obtain the yrast and yrare states by using (11), (14) and (15). The nuclear states with lower energy E^J (in (14)) constitute the yrast band whereas those with higher energy E^J form the yrare band. It should be pointed out here that the neutron pair in $i_{13/2}$ orbit also plays an important role in the present calculations performed in the framework of VAP formalism. The neutron occupancies vary with deformation β which changes gradually with J. It is found in ^{154}Gd that the intrinsic states for $J < 8$ are characterised by only one pair of neutrons in $i_{13/2}$ orbit with $\Omega = \pm 1/2$, whereas the intrinsic states for $J \geqslant 8$ have two pairs of neutrons in $i_{1/32}$ orbit with $\Omega = \pm 1/2$ and $\Omega = \pm 3/2$ substates. The occupation changes from the $h_{11/2}$ neutron state with $\Omega = 11/2$ for $J < 8$ to the $i_{13/2}$ neutron state with $\Omega = 3/2$ for $J \geqslant 8$.

The relationship of the present VAP method with the phenomenological RAL model (Stephens and Simon 1972) can now be explored by considering two bands g_1 and g_2 obtained from the intrinsic states of the nucleus. The g_1 band is constructed on the intrinsic state corresponding to $J=0^+$ state and g_2 band is constructed from the intrinsic state corresponding to $J=12^+$ state in ^{154}Gd. The projected spectra of these two bands g_1 and g_2 in ^{154}Gd are shown in table 1. It is found that the two bands cross and the energies $E^J(g_1)$ for $J<10$ and $E^J(g_2)$ for $J\geqslant 10$ are very close to those obtained from the ground band. Thus the ground band states with $J<10$ correspond to g_1 band whereas the ground band states with $J\geqslant 10$ correspond to g_2 band characterised by the occupancy of an extra pair of neutron in $i_{13/2}$ orbit with $\Omega=3/2$. To investigate the alignment effect, we have calculated the J-content p^J in the g_1 and g_2 bands. The results in table 1 indicate that p^J for states with $J<10$ ($J\geqslant 10$) is substantially larger in g_1 (g_2) band than in g_2 (g_1) band. Thus the alignment of a pair of neutrons in $i_{13/2}$ orbit as in g_2 band gives rise to the yrast states with $J\geqslant 10$ in ^{154}Gd. Our calculations in ^{156}Gd, however, do not indicate such an effect.

The energy spectra obtained from the bands built on ϕ_0 (f) and ϕ_0 (f') of (10) are found to be nearly degenerate, indicating the need for the band-mixing formulation. The two bands are mixed using the band-mixing formulation of (14) and (15). The results of the band-mixing calculations in ^{154}Gd and ^{156}Gd are discussed below.

3.1 ^{154}Gd

The results of the band-mixing calculations in ^{154}Gd are shown in tables 2 and 3. The calculated renormalised energy E^J_{norm} and the experimental energy E^J_{exp} for each angular momentum state J in both the bands of ^{154}Gd are displayed in table 2. The values of the variational parameters β, Δ_p, and Δ_n corresponding to the minimum in energy of each state are also shown in table 2. It is seen from table 2 that the

Table 1. The calculated energies (in MeV) E^J and the J-contents p^J are tabulated for each angular momentum state J in the ground, g_1 and g_2 bands for ^{154}Gd. These energies are not renormalised.

J	ground band		g_1 band		g_2 band	
	E^J	p^J	E^J	p^J	E^J	p^J
0	0·00	0·04	0·00	0·04	1·52	0·01
2	0·28	0·16	0·27	0·16	1·58	0·07
4	0·85	0·22	0·92	0·22	1·72	0·11
6	1·47	0·21	1·77	0·21	1·95	0·14
8	2·07	0·15	2·67	0·16	2·25	0·15
10	2·62	0·14	3·60	0·10	2·63	0·14
12	3·10	0·12	4·91	0·05	2·90	0·12
14	3·63	0·09	7·25	0·02	3·64	0·09
16	4·24	0·07	11·05	0·01	4·25	0·07
18	4·92	0·04	11·67	0·01	4·94	0·04

Table 2. The calculated and experimental energies (in MeV) E^J_{norm} and E^J_{exp} are tabulated for each angular momentum state J in the two bands of ^{154}Gd. The deformation parameter β, the proton pairing gap Δ_p and the neutron pairing gap Δ_n are shown in columns 2, 3 and 4 respectively.

J	β	Δ_p (MeV)	Δ_n (MeV)	yrast band		yrare band	
				$E^{J\dagger}_{\text{exp}}$	E^J_{norm}	$E^{J\dagger}_{\text{exp}}$	E^J_{norm}
0	0·26	1·10	0·89	0·00	0·00	0·68	0·74
2	0·26	1·10	0·89	0·12	0·12	0·82	0·85
4	0·28	1·05	0·84	0·37	0·39	1·05	1·09
6	0·32	1·03	0·80	0·72	0·78	1·37	1·33
8	0·35	0·96	0·55	1·14	1·22	1·76	1·75
10	0·35	0·91	0·32	1·64	1·67	2·20	2·20
12	0·35	0·89	0·00	2·19	2·25	2·62	2·61
14	0·35	0·82	0·00	2·78	2·88	3·03	3·04
16	0·35	0·82	0·00	3·40	3·37	3·49	3·51
18	0·35	0·73	0·00	4·02	3·92	4·08	4·08

†Sayer *et al* (1975)

Table 3. The calculated and the experimental $B(E2; J \to J-2)$ values for the yrast band and the ratios $B(E2; J' \to J-2)/B(E2; J' \to J'-2)$ for the cross-band transitions are tabulated for ^{154}Gd. The primed and unprimed values of J correspond to the yrare and yrast states respectively.
The last line gives the ratio $B(E2; 18 \to 16')/B(E2; 18 \to 16)$.

J	$B(E2; J \to J-2)e^2b^2$		$\frac{B(E2; J' \to J'-2)}{B(E2; J' \to J'-2)}$	
	Calc.	Expt.†	Calc.	Expt.††
2	0·72	0·78	$2{\cdot}4 \times 10^{-4}$	$2{\cdot}5 \times 10^{-3}$
4	1·07	1·18	$7{\cdot}2 \times 10^{-4}$	$8{\cdot}0 \times 10^{-3}$
6	1·15	1·38	$2{\cdot}0 \times 10^{-4}$	$1{\cdot}5 \times 10^{-3}$
8	1·66	1·53	$1{\cdot}0 \times 10^{-3}$	3×10^{-3}
10	1·74	1·73	$1{\cdot}2 \times 10^{-3}$	$0{\cdot}73 \times 10^{-3}$
12	1·86	—	$3{\cdot}4 \times 10^{-4}$	$6{\cdot}3 \times 10^{-4}$
14	1·91	—	$1{\cdot}5 \times 10^{-3}$	$< 3 \times 10^{-3}$
16	1·88	—	$1{\cdot}5 \times 10^{-2}$	$3{\cdot}6 \times 10^{-2}$
18	—	—	2·4	1·35
18	—	—	2·7	1·66

†Ward *et al* 1975
††Khoo *et al* 1973

deformation β goes on gradually increasing from 0.26 to 0.35 as angular momentum J increases from 0 to 8 and then remains constant for all the states with $J \geqslant 8$. The pairing gap Δ_p for protons decreases slowly with increasing J from the value 1.10 MeV for $J=0$ to the value 0.73 MeV for $J=18$. The neutron pairing gap Δ_n first decreases gradually from the value 0.89 MeV for $J=0$ to 0.80 MeV for $J=6$ and then starts decreasing drastically. The neutron pairing gap vanishes at $J=12$ and remains zero for all the higher angular momentum states with $J \geqslant 12$. The calculated energies

of the yrast band states are renormalised as discussed in § 2·3 by using the value $I_{core} = 13\ \hbar^2/\text{MeV}$ for $J \leqslant 12$ and $I_{core} = 8\ \hbar^2/\text{MeV}$ for $J > 12$. The relative energy separations in the yrare band are not renormalised. However, the calculated energy of the 0^+ state of the yrare band is renormalised by employing the same value $I_{core} = 13\ \hbar^2/\text{MeV}$ as in the case of yrast band and the value of I^J_{calc} corresponding to the energetically close state ($J^\pi = 6^+$) in the yrast band. It is seen from the results in table 2 that the renormalised energies of all the states in the yrast and yrare bands are in good agreement with the corresponding experimental energies (Khoo *et al* 1973). This agreement is obtained with essentially two values of the parameter I_{core}. Different values for the two sets of states in ^{154}Gd can be understood in view of the discussion in § 2.3.

The energies E^J_{norm} are plotted as function of $J(J+1)$ in figure 1. It can be seen from figure 1 that, the energies of the states with $J = 14'$, $16'$ and 18 lie on a straight line, which intersects the straight line passing through the energies of states with $J = 14$, 16 and $18'$. The primed and unprimed states belong to yrare and yrast bands respectively. The intersection point of these two straight lines is between $J = 16$ and $J = 18$ in agreement with the experimental observation (Khoo *et al* 1973). The present band-mixing calculations show that the structure of $J = 18'$ state is similar to that of $J = 14$ and 16 states and the structure of $J = 18$ state is similar to that of $J = 14'$ and $16'$ states. The structure of the band-mixed wave functions for the yrast and yrare states is described by the sign of the band-mixing coefficient B^J of equation (15). The sign of this band-mixing coefficient is opposite for the state with same J in yrast and yrare band. Our calculations yield the same sign of the band-mixing coefficients for all the yrast

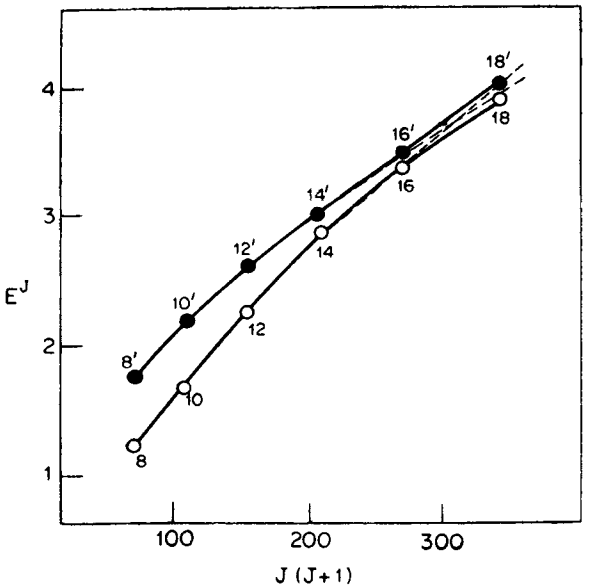

Figure 1. Energy levels E^J of the yrast and yrare bands are plotted against $J(J+1)$. The primed and unprimed J values correspond to the yrare and yrast states respectively.

states from $J = 0'$ to $J = 16$ and for the yrare state $J = 18'$. The sign of the band-mixing coefficient is also found to be the same for all the yrare states from $J' = 0'$ to $J' = 16'$ and the yrast state $J = 18$. This clearly indicates that the structure of $J' = 18'$ state is similar to that of the states with $J = 0$ to 16 whereas the structure of $J = 18$ state is similar to those with $J' = 0'$ to $J' = 16'$. Thus the present microscopic calculations explain the observed (Khoo *et al* 1973) band-crossing between $J = 16$ and $J=18$.

The calculated quadrupole moment $Q(J)$ and the intrinsic quadrupole moment $Q_0(Q)$ and $Q_0(E2)$ extracted from (18) and (19) are shown in table 4. It is seen from table 4 that the values $Q_0(Q)$ and $Q_0(E2)$ increase with J to reach the value corresponding to that of a rigid rotator.

The interband and intraband $B(E2)$ values are calculated using the effective charges employed by Kumar and Baranger (1968). The calculated and the experimental $B(E2)$ values for the intraband and interband $E2$ transitions are tabulated in table 3. It is seen from table 3 that the calculated intraband $B(E2)$ values are in good agreement with the corresponding experimental values (Ward *et al* 1975). The calculated values of the ratio $B(E2; J' \rightarrow J-2)/B(E2; J' \rightarrow J'-2)$ for the interband and intraband $E2$ transitions are in good agreement with experimental values (Khoo *et al* 1973) except $J \leqslant 6$. The observed (Khoo *et al* 1973) characteristic feature of sudden increase in the value of this ratio at $J' = 18'$ is correctly reproduced by our calculations. Moreover our calculations also give nearly the same value for the ratios $B[E2; 18 \rightarrow 16']/B[E2; 18 \rightarrow 16]$ and $B(E2; 18' \rightarrow 16)/B[E2; 18' \rightarrow 16']$ as is experimentally observed (Khoo *et al* 1973). This near equality of the two ratios also suggests the band-crossing between $J=16$ and $J=18$.

Finally, the yrare band shows a backbending at $J=12$ whereas the yrast band exhibits the same phenomenon at $J=16$ (Khoo *et al* 1973). The calculated energies shown in table 2 also indicate backbending in the yrast band at $J=14$ and in the yrare band at $J=10$ as can be seen from successive energy differences. The sudden vanishing of Δ_n at $J=12$ may be partly responsible for the observed backbending in ^{154}Gd. The sudden change in the occupation of $i_{13/2}$ neutron orbitals in the intrinsic states

Table 4. The calculated static quadrupole moment $Q(J)$ and the intrinsic quadrupole moments $Q_0(Q)$ and $Q_0(E2)$ extracted from the computed $Q(J)$ and $B(E2)$ values respectively, for the yrast bands of $^{154, 156}$Gd are tabulated. The tabulated quantities are in units of eb.

J	^{154}Gd			^{156}Gd		
	$-Q(J)$	$Q_0(Q)$	$Q_0(E2)$	$-Q(J)$	$Q_0(Q)$	$Q_0(E2)$
2	1·72	6·03	6·02	1·94	6·80	6·36
4	2·31	6·36	6·14	2·69	7·40	6·62
6	2·79	6·97	6·06	2·96	7·73	6·74
8	3·12	7·41	6·71	3·25	7·75	6·85
10	3·25	7·49	7·19	3·37	7·75	6·83
12	3·35	7·54	7·37	3·44	7·78	7·71
14	3·41	7·56	7·63	3·52	7·76	7·76
16	3·45	7·55	7·83			
18	3·47	7·51				

for high spin states also plays an important role in backbending. The present microscopic calculations show clearly that the alignment of a pair of neutrons in $i_{13/2}$ orbit with $\Omega=3/2$ gives rise to the high spin states with $J \geqslant 10$. The change in occupation probability along with the alignment effect in $i_{13/2}$ neutron orbitals results in backbending observed in ^{154}Gd. This conclusion can be corroborated by the fact that such an effect is found to be absent in ^{156}Gd which does not manifest backbending.

3.2 ^{156}Gd

The results of the band-mixing calculations in ^{156}Gd are shown in tables 5 and 6. The calculated renormalised energy E^J_{norm} and the experimental energy E^J_{exp} for each angular momentum state J in both the bands in ^{156}Gd are displayed in table 5. The values of the variational parameters β, Δ_p and Δ_n corresponding to the minimum in energy of each state are also shown in table 5. It is seen from table 5 that the defor-

Table 5. The calculated and experimental energies (in MeV) E^J_{norm} and E^J_{exp} are tabulated for each angular momentum state J in the two bands of ^{156}Gd. The deformation parameter β, the proton pairing gap Δ_p and the neutron pairing gap Δ_n are shown in columns 2, 3 and 4 respectively.

J	β	Δ_p (MeV)	Δ_n (MeV)	yrast band		yrare band	
				$E^{J\dagger}_{\text{exp}}$	E^J_{norm}	$E^{J\dagger}_{\text{exp}}$	E^J_{norm}
0	0·30	1·05	0·90	0·00	0·00	1·05	1·04
2	0·30	1·05	0·90	0·09	0·09	1·13	1·14
4	0·34	0·96	0·81	0·29	0·32	1·30	1·30
6	0·34	0·96	0·81	0·59	0·62	—	1·56
8	0·36	0·82	0·56	0·97	1·02	—	2·05
10	0·36	0·78	0·52	1·42	1·43	—	2·52
12	0·36	0·78	0·52	1·92	1·88	—	3·06
14	0·36	0·78	0·29	2·47	2·38	—	3·70
16	0·36	0·78	0·00	3·06	2·94	—	4·40

†Sayer *et al* (1975)

Table 6. The calculated and experimental $B(E2; J \rightarrow J-2)$ values for the yrast band in ^{156}Gd are tabulated.

J	$B(E2; J \rightarrow J-2)\ e^2b^2$	
	Expt.†	Calc.
2	0·92	0·92
4	1·29	1·44
6	1·47	1·66
8	1·57	1·83
10	1·59	1·94

†Sie *et al* (1977)

mation β goes on gradually increasing from 0·30 to 0·36 as angular momentum J increases from 0 to 8 and remains constant for all states with $J \geqslant 8$. The pairing gap Δ_p for protons decreases slowly with increasing J from the value 1.05 MeV for $J=0$ to the value 0·78 MeV for $J=16$. The neutron pairing gap Δ_n decreases gradually from the value 0·90 MeV for $J=0$ to 0·81 MeV for $J=6$ and then starts decreasing drastically. The neutron pairing gap vanishes at $J=16$. As mentioned earlier, the change of neutron occupancy found at $J=8$ in ^{154}Gd, does not take place in ^{156}Gd. The calculated energies of the yrast band states are renormalised as discussed in §2.3 by using the value $I_{\text{core}}=16\hbar^2/\text{MeV}$. It is worthwhile to point out that only a single value of I_{core} suffices for all the states of yrast band. This may be connected to the fact that in ^{156}Gd, there are no changes of neutron occupancy, as in ^{154}Gd where two values of I_{core} were necessary for the yrast states. The relative energy separations of the yrare band are not renormalised. However, the 0^+ state of the yrare band is renormalised using $I_{\text{core}}=3\hbar^2/\text{MeV}$ and the value I^J_{calc} corresponding to the energetically close state ($J^\pi=8^+$) in the yrast band. It is seen from the results in table 5 that the renormalised energies of all states in the yrast and yrare bands are in good agreement with corresponding experimental energies (Sayer *et al* 1975). This agreement is obtained essentially with two values of the parameter I_{core}. The different values for the two bands in ^{156}Gd and the difference of these values from those in ^{154}Gd can be understood in view of the discussion in §2.3.

The interband and intraband $B(E2)$ values are calculated by using effective charges employed by Kumar and Baranger (1968). The calculated and the experimental $B(E2)$ values for the intraband $E2$ transitions are tabulated in table 6. It is seen from table 6 that the calculated intraband $B(E2)$ values are in good agreement with the corresponding experimental values (Sie *et al* 1977). The interband $E2$ transitions are also reasonably well explained by our calculations. The calculated values of $B(E2;\ 2'\rightarrow 0)/B(E2;\ 2'\rightarrow 2)$, $B(E2;\ 4'\rightarrow 2)/B(E2;\ 4'\rightarrow 4)$ and $B(E2;\ 4'\rightarrow 2)/B(E2;\ 4'\rightarrow 6)$ are 0·14, 0·40 and 0·30 as compared to the corresponding experimental values (Sie *et al* 1977) 0·18, 0·19 and 0·55 respectively.

The calculated quadrupole moment $Q(J)$ along with the intrinsic quadrupole moments $Q_0(Q)$ and $Q_0(E2)$ extracted from equations (18) and (19) are shown in table 4. The Q_0 values are nearly constant.

4. Conclusions

A microscopic band-mixing formalism of variation after projection of angular momentum and conservation of nucleon number is applied to study the yrast and yrare bands in ^{154,156}Gd. The nuclear Hamiltonian employed in the calculations consists of quadrupole plus pairing interactions. The configuration space comprises two major shells for both protons and neutrons outside the inert core with $Z=40$ and $N=70$. The effects of core polarisation and configuration truncation are simulated by ascribing effective charges to the nucleons and by introducing moment of inertia of the core to renormalise the energy spectra. The calculated energy spectra and the intraband and interband $B(E2)$ values are in good agreement with the corresponding experimental data. Our calculations in ^{154}Gd show that there is a sudden change in the occupation of neutron orbitals in

the intrinsic structure of the nucleus. The intrinsic states for $J \geqslant 8$ are characterised by an additional pair of neutrons in $i_{13/2}$ orbit with $\Omega = \pm 3/2$. The observed backbending in ^{154}Gd is probably due to this change in the occupation probability of the $i_{13/2}$ neutron orbital with $\Omega = \pm 3/2$. It is also shown that the alignment of a pair of neutrons in this $i_{13/2}$ orbit gives rise to the states with $J \geqslant 10$ in ^{154}Gd. The present calculations do not indicate any change in the occupation of neutron orbitals in the intrinsic structure of ^{156}Gd and this may be the reason why it does not manifest backbending.

References

Banerjee B, Mang M and Ring P 1973 *Nucl. Phys.* **A215** 366
Das Gupta S and Preston M A 1963 *Nucl. Phys.* **49** 401
Faessler A, Grummer F, Lin L and Urbano J 1974 *Phys. Lett.* **B48** 87
Grummer F, Schmid K W and Faessler A 1975 *Nucl. Phys.* **A239** 289
Gunye M R, Das Gupta S and Preston M A 1964 *Phys. Lett.* **13** 246
Gunye M R and Warke C S 1979 *Phys. Rev.* **C20** 372
Khoo T L, Bernthal F M, Boyno J S and Warner A 1973 *Phys. Rev. Lett.* **18** 1146
Krumlinde J and Szymanski Z 1974 *Phys. Lett.* **B53** 322
Kumar K 1972 *Phys. Scr.* **6** 270
Kumar K and Baranger M 1968 *Nucl. Phys.* **A110** 529
Mottelson B R and Valatin J G 1960 *Phys. Rev. Lett.* **5** 511
Nair S C K and Ansari A 1973 *Phys. Lett.* **B47** 200
Sayer R O, Smith J S III and Milner W T 1975 *Atomic data and nuclear data tables* **15** 85
Sie S H, Ward D, Geiger J S, Graham R L and Andrews H R 1977 *Nucl. Phys.* **A291** 443
Stephens F S and Simon R S 1972 *Nucl. Phys.* **A183** 257
Ward D H, Andrews H R, Geiger J S, Graham R L and Sie S H 1975 *Bull. Acad. Sci. USSR* **39** 36
Warke C S and Gunye M R 1975 *Phys. Rev.* **C12** 1647
Warke C S and Gunye M R 1976 *Phys, Rev.* **C13** 859